Crowded Field Photometry with Deconvolved Images

P. Linde and S. Spännare,
Lund Observatory,
Box 43,
S-221 00 Lund, Sweden

June 18, 1993

Abstract

A local implementation of the Lucy-Richardson algorithm has been used to deconvolve a set of crowded stellar field images. The effects of deconvolution on detection limits as well as on photometric and astrometric properties have been investigated as a function of the number of deconvolution iterations. Results show that deconvolution improves detection of faint stars, although artifacts are also found. Both automatic and interactive detection methods benefited. However, the interactive method always gave the better results. Regarding astrometry, deconvolution provides more stars measurable without significant degradation of positional accuracy. The photometric precision is affected by deconvolution in several ways. Errors due to unresolved images are notably reduced while flux redistribution between stars and background increases the errors.

1 Introduction

Crowded field photometry has for the last decade opened up new possibilities to study many classes of astronomical objects, characterised by overlapping stellar images. However, the available techniques are still imperfect in some respects. One of the limitations is the difficulty to detect all components in a group of overlapping stellar images. An interesting approach to overcome this difficulty is to employ deconvolution techniques in order to reduce the overlapping. A series of tests have therefore been performed to evaluate the effects of deconvolution on crowded fields. Three aspects have been investigated, detectability and effects on positional and intensity measurements. Some initial results are presented here.

2 Simulations

Simulated stellar fields were created for the tests. Fig. 1 shows one example. This simulation reproduces a typical star field in the Large Magellanic Cloud, as seen with the 2.2m ESO telescope. The field is characterised by a high degree of overlapping, a generally low signal-to-noise ratio and a poor resolution (FWHM = 2.5 arcsec). Stars in the magnitude interval V=16.6 to V=22 are represented in the image. These magnitudes correspond to integrated intensities from 37000 to 250 ADU (1 Analogue-to-Digital Unit = 11 photons) and maximum intensities of 650 to 4 ADU above the background level. The noise in the background was 5 ADU. Thus, many faint stars were hidden in the background noise. The total number of simulated stars was 1282.

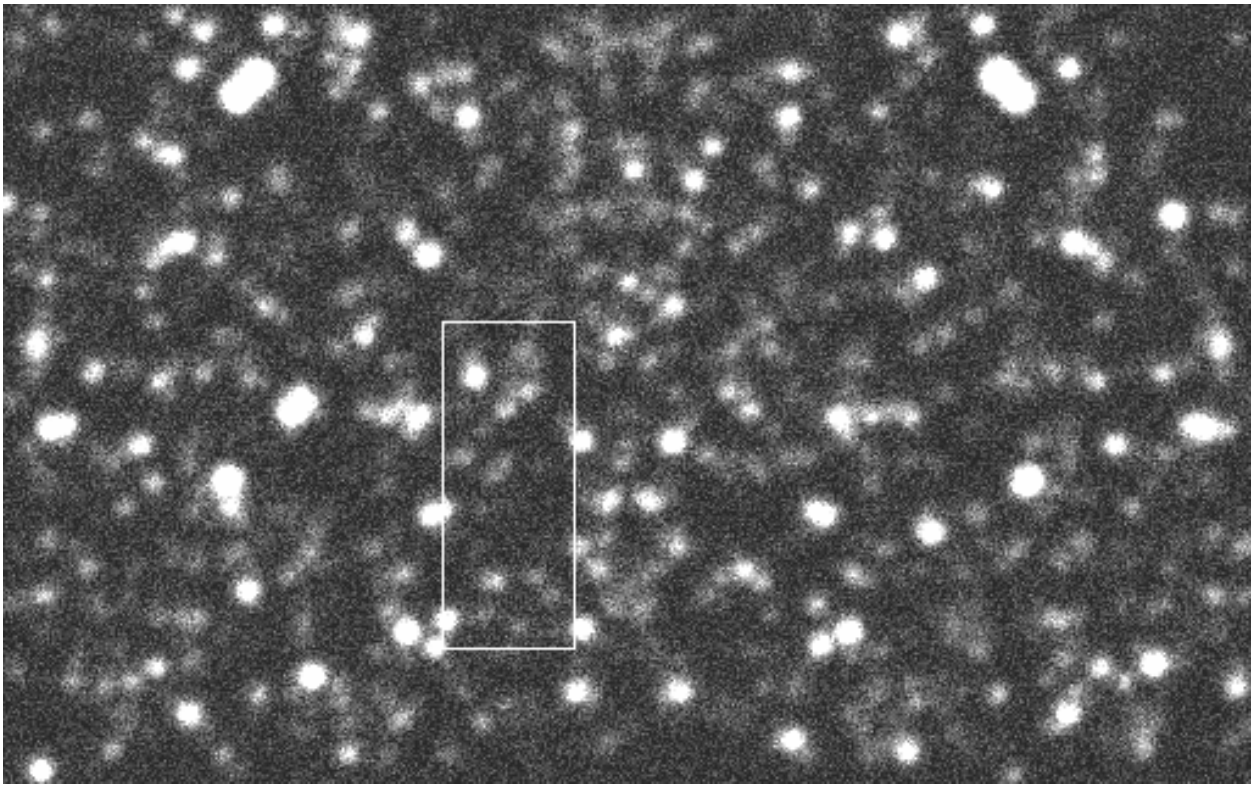

Figure 1: A simulated stellar field used in the tests. The marked area is shown in detail in Fig. 2.

3 Detection

A local implementation of the Lucy-Richardson (Lucy, [4]) algorithm was used in the tests. The implementation was compared to the version available in MIDAS and found to give very similar results. The test image was subsequently deconvolved using up to 100 iterations and a digital movie was produced with each iteration constituting a separate frame. This allowed a close inspection of various effects in the deconvolution process. Fig 2a shows a subsection of the test image in Fig 1. Dark circles mark the known positions of stars. Fig 2b shows the same subsection after 20 iterations of deconvolution.

During the 100 iterations, the resolution increased from 2.5 arcsec to 0.9 arcsec. Most of the increase was seen during the first 20 iterations. On the other hand, convergence was still not reached after 100 iterations. Comparing Fig. 2a with Fig. 2b, it is obvious that all stars are more visible. However, other effects are also noted. In Fig. 2b, it is seen that flux is redistributed from the background into the star images. This affects the photometric precision that can be reached.

Faint star-like artifacts begin to appear at positions where no stars exist. To further investigate this phenomenon, a second test image was made, containing a different original noise pattern. The result after 20 iterations is seen in Fig. 2c, which shows the same subsection as in Fig. 2a and b. Similar artifacts have been created but they are located at positions different from those in Fig 2b.

To estimate in more quantitative terms the impact of deconvolution on star detection, two different search techniques were employed to determine the number of objects in the images based on 0, 10, 20 and 100 iterations. One utilised an interactive computer-aided approach (Linde [3]), while the other used the automatic search mode of the ROMAFOT program (Buonanno et al., [1]). To qualify as a true detection, the object must not only be detected but also measured and approved as a star by the corresponding measuring program. The results are shown in Fig. 3a and b as function of magnitude, while Table 1 summarises the total number of stars that were found. It is seen that both methods benefit from deconvolution of the investigated image. ROMAFOT exhibited an anomalous behaviour for the zero iteration image and generally detected fewer objects.

A complication for correctly identifying stars is the creation of artifacts. Since the deconvolution

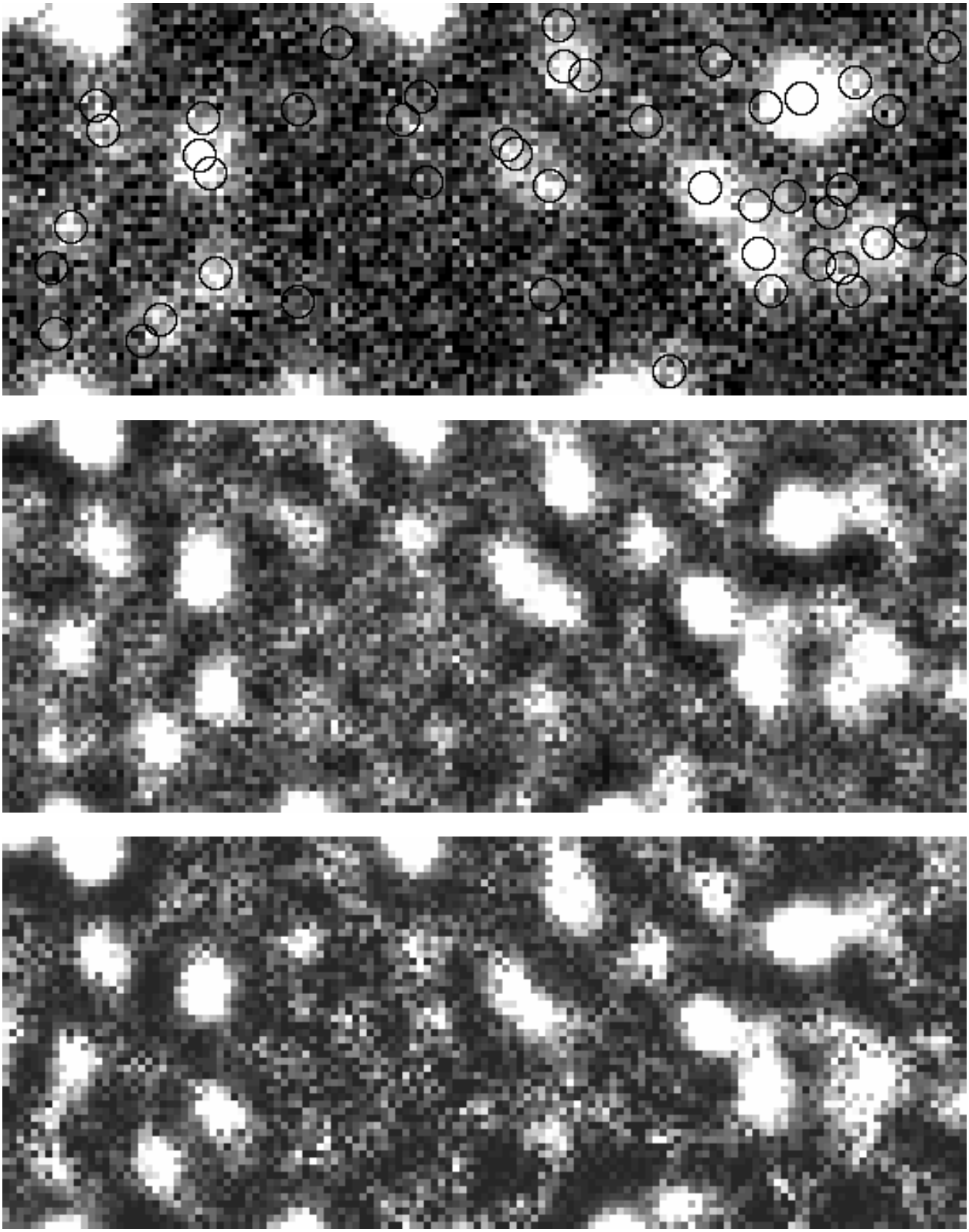

Figure 2: (a) (top panel): A subsection of the test image. The circles mark known positions of stars. (b) (centre panel): The same subsection after 20 iterations of Lucy-Richardson deconvolution. Several star-like artifacts appear near the centre. (c) (bottom panel): The same as (b), but with different noise pattern. The artifacts are at positions different from those in (b).

No. of iter.	Interactive method		Automatic method	
	Stars	Artifacts	Stars	Artifacts
0	514	19	106	30
10	645	57	416	47
20	708	198	490	45
100	776	722	660	375

Table 1: The total of found stars and artifacts, using two different searching techniques.

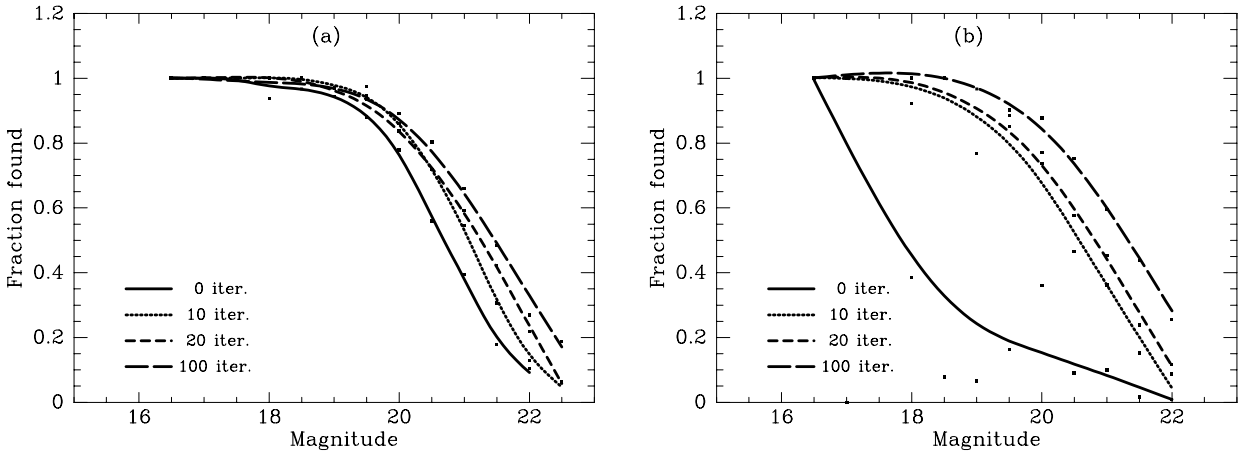

Figure 3: Fraction of identified stars as function of magnitude and number of deconvolution iterations. (a) shows the results of the interactive identification, while (b) shows the results using an automatic searching method (ROMAFOT).

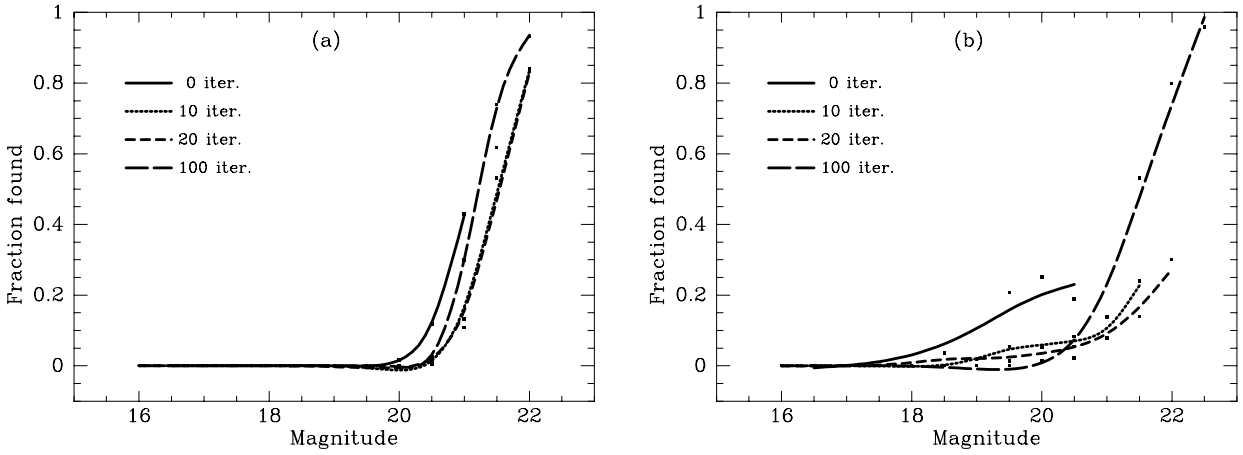

Figure 4: Fraction of found artifacts as function of magnitude and number of deconvolution iterations. (a) shows the results of the interactive identification, while (b) shows the results using an automatic searching method (ROMAFOT).

tends to force the shape of the point spread function on random structures, artifacts usually look like stars (see Fig. 2). Fig. 4 shows how the fraction of artifacts increases with magnitude and the accumulated numbers are given in Table 1. It can be noted that the number of artifacts rises quite sharply for the 100 iteration image. For this type of image and application, 10-20 iterations is a reasonable number.

4 Astrometric and photometric behaviour

The astrometric behaviour is illustrated in Fig. 5, where the measured positions have been compared to the known positions. Fig. 5a shows the result for 0 iterations and 5b for 20 iterations. No systematic effect is seen, and although 35 % more (faint) stars were detected in the 20 iteration case, the spread is about the same.

The photometric behaviour is shown in Fig. 6. Measured magnitudes have been compared to known magnitudes, for (a) the 0 iteration case and (b) the 20 iteration case. It is noted that the spread is considerable already in the non-deconvolved image. A systematic tendency for overestimating the intensities is seen, both for some individual cases at brighter magnitudes, and as a more general trend at fainter magnitudes. This effect is mostly due to the confusion problem, where very close stars have mistakenly been measured as single objects. However, after deconvolution the increased resolution has permitted decomposition of many such instances, which is indicated by the more linear behaviour in Fig. 5b. The general spread is slightly larger in 5b, which however contains 43 additional faint stars.

5 Conclusions

It is clear that Lucy-Richardson deconvolution greatly improves identification of stars in crowded fields, independent of the search technique used. The number of artifacts also increases, but provided that the number of iterations is adequately limited and several exposures can be cross-correlated, this problem can be eliminated. The quantitative behaviour for deconvolved images is good regarding the positional precision. The photometric results are not entirely conclusive. However, in our case, using low signal-to-noise ratio data, the results are encouraging. The flux redistribution problem typical of many deconvolution techniques is *not* the major contributor to the errors. On the contrary, systematic effects due to image confusion are notably reduced by applying deconvolution. However, the currently recommended procedure, in agreement with Cohen [2], would be to use detection data from deconvolved images and apply them to photometric measurements of the original image.

References

[1] Buonanno, R., Buscema, G., Corsi, C.E., Ferraro, I. and Iannicola, G.: 1983 *Astron. Astrophys.* **126**, 278-282

[2] Cohen, Judith G.: 1991 *Astron. J.* **101**, 734-737

[3] Linde, P.,: 1989 *Proceedings of 1st ESO/ST-ECF Data Analysis Workshop*, P Grosbøl, F Murtagh, R Warmels (eds), 201-204, 1989.

[4] Lucy, L.B.: 1974 *Astron. J.* **79**, 745-754

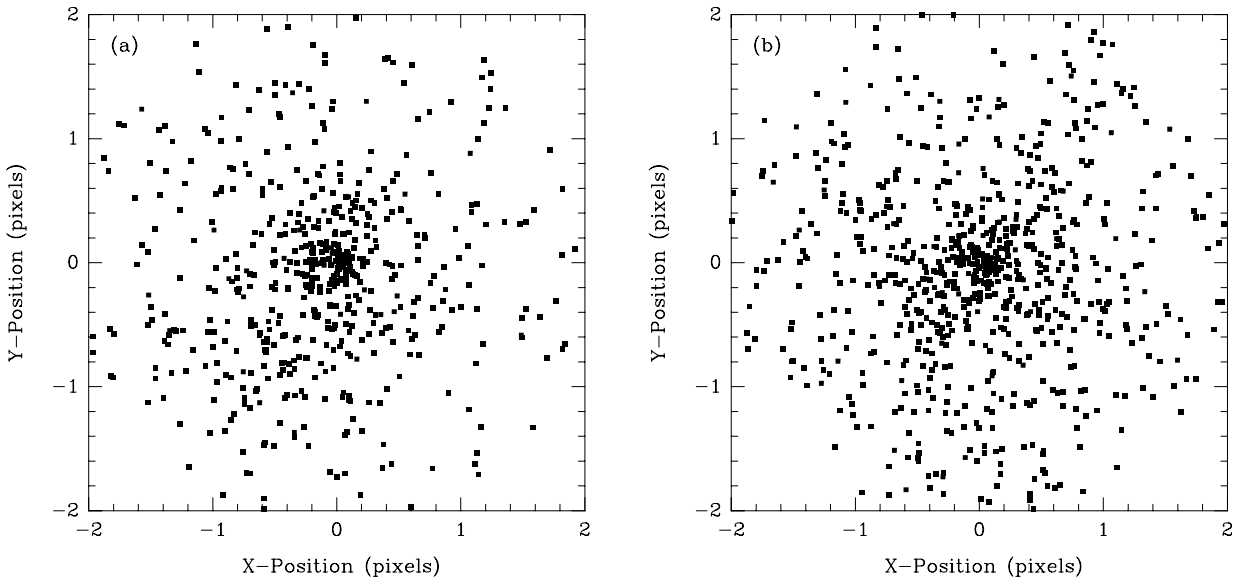

Figure 5: Results of the astrometry test. (a) shows measurements on the original image (545 stars, $\sigma = 0.75$ pixels), (b) shows measurements on an image deconvolved using 20 iterations (737 stars, $\sigma = 0.78$ pixels).

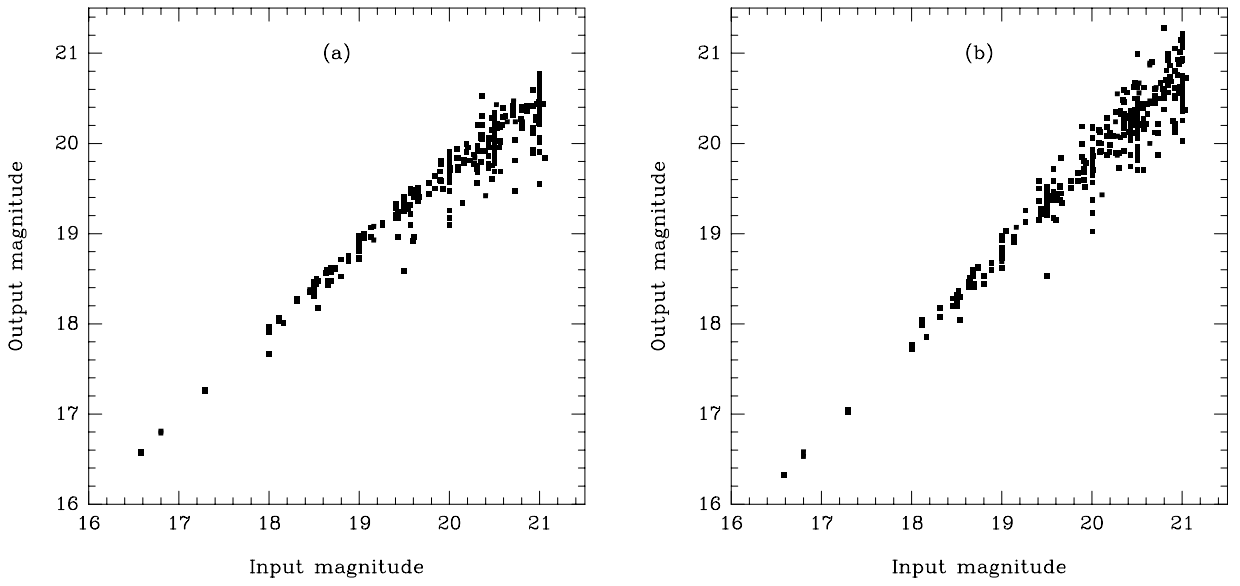

Figure 6: Results of the photometry test. (a) shows measurements on the original image (307 stars), (b) shows measurements on an image deconvolved using 20 iterations (350 stars).